# Quantitative Histology of Contused Lung Tissue with Comparison to Computed Tomography

F. S. Gayzik[1,2], J. J. Hoth[1,2], N. Brownlee[1] and J.D. Stitzel[1,2]
[1]Wake Forest University School of Medicine;
[2]Virginia Tech – Wake Forest University Center for Injury Biomechanics

## ABSTRACT

*This study presents an image analysis algorithm for quantifying the volume fraction of pathology in serial histology of the rat lung. The right lung of male Sprague-Dawley rats (n=4) was contused using a controlled insult applied via an instrumented, electronic piston. The right (struck) and left lungs were excised at 48 hours post-insult, fixed in 10% formalin. Serial histology was taken at 1.5 mm intervals on the struck lung and 3 mm intervals on the left lung. Sections were stained with H&E and digitally imaged using a fixed, high-resolution digital camera. Immediately prior to sacrifice, computed tomography images of all subjects were also acquired. An automated image analysis program was applied to each image (8-bit, RGB) using morphological (dilatation and erosion), filtering (circular averaging), and thresholding techniques to sort pixels representing healthy lung tissue, pathologic lung tissue, and blood into separate masks. Blood was determined by multi-channel thresholding in the following inclusive ranges: Red (197-240), Green (0-90) and Blue (115-154). After applying the morphological and filtering operations, lung pathology was identified as all pixels exceeding a grayscale value of 85, with 0 being black and 255 being white. The average normalized volume of pathology across the data set was 12.63 ± 11.40 %. The results showed greater volumes of tissue pathology than blood in all subjects indicating a good model for blunt lung trauma. CT segmentation data from the same four animals was used for a related study but was included for the purposes of comparison. These values were determined through a semi-automated approach and resulted in an average pathology volume of 16.92 ± 9.66 %. Normalized pathology did not differ significantly between histology and CT ($p = 0.18$, paired t-test for sample means, $\alpha = 0.05$). The histology analysis algorithm and CT data resulted in similar trends across the data set. This approach can be used to improve the accuracy of both histology-based and CT-based segmentation processes.*

## INTRODUCTION

In this study, digital histology analysis is used to quantify the extent of pulmonary contusion (PC) following a thoracic insult. Thoracic injuries are exceedingly common in blunt trauma patients and are associated with significant morbidity and mortality. (Cohn, 1997; Blansfield, 1999) Contusion volume at the time of hospitalization has been shown to be an independent predictor for the development of Acute Respiratory Distress Syndrome (ARDS), with the risk of ARDS increasing sharply with PC in excess of 20% by volume. (Miller, 2001) Computed tomography (CT) is the most frequently used clinical modality for obtaining volumetric lung contusion data, however the segmentation process is labor intensive and can be confounded by differing types of pathology that produce image data within the same Hounsfield unit (HU) range. This research presents an image analysis algorithm for the automated identification of lung contusion applied to serial histology sections of the rat lung. The long-term goal of this research is to use histologically-calculated contusion volume as a standard against which CT-calculated contusion volume can be validated.

## METHODS

All experimental protocols were approved by the Wake Forest School of Medicine Animal Care and Use Committee. Contusion was generated in Sprague-Dawley male rats (n = 4) using an instrumented, electromagnetically-driven piston, with a nominal impact speed and penetration depth of 5 m $s^{-1}$ and 6.3 mm respectively. The right lung was exposed via thoracotomy, and was directly struck with the piston. Force and displacement data were collected for each impact. (Stitzel, 2005; Gayzik, 2007B) Detailed descriptions of the experimental preparation are available in the literature (Stitzel, 2005; Hoth, 2006; Gayzik, 2007B) At 48 hours post impact, CT images were acquired and the subjects were euthanized for histology. The intact lungs were excised and fixed in 10% buffered formalin at a pressure of 15mm $H_20$ prior to sectioning. Specimens were embedded in paraffin, sectioned, and stained with hematoxylin and eosin (H&E) for examination. The right (struck) lung was sectioned at $\Delta$= 1.5 mm intervals, and the left lung was sectioned at $\Delta$= 3 mm intervals.

The histological specimens were digitally imaged using a rigidly-mounted Fuji S3 105 mm digital camera equipped with a micro-nikkor lens (Fuji, Valhalla, NY; Nikon, Melville, NY). A metric ruler with clear millimeter demarcations was imaged under the same protocol to determine the resolution of the resulting data. All images were saved at high-resolution, resampled to 1064 x 712 pixels, and saved as bitmapped images via a batch process. Resampled images were imported to Matlab (The MathWorks, Natick, MA) as unsigned, 24-bit, RGB images for preprocessing and segmentation. The segmentation algorithm and accompanying graphical user interface used were written in house.

Images were preprocessed to: 1. clearly distinguish background pixels from lung pixels and 2. translate each so that they were aligned along a common centroid. To accomplish these tasks, the green channel of the image was used because it exhibited the greatest contrast between lung pixels and background pixels, and reduced the computational cost. The monochrome image

was converted to binary format and several Matlab image processing functions were employed. Binary format was advantageous since black (0) and white (1) could be used to represent background and lung masks. Because of the porous nature of lung tissue, the *imfill* command was used to ensure that regions of pixels representing alveolar airspace were not considered background pixels. The *regionprops* command was used to identify boundaries of lung tissue and calculate the centroid (analogous to center of mass) of each region of lung tissue. In cases where more than one distinct region of lung tissue was present in a single slide, a weighted average of the centroids based on the region size was used to determine a single image centroid. Images were then translated to align the entire stack along the centroid. Preprocessing was done separately for the right and left lung. This process is shown in Figure 1.

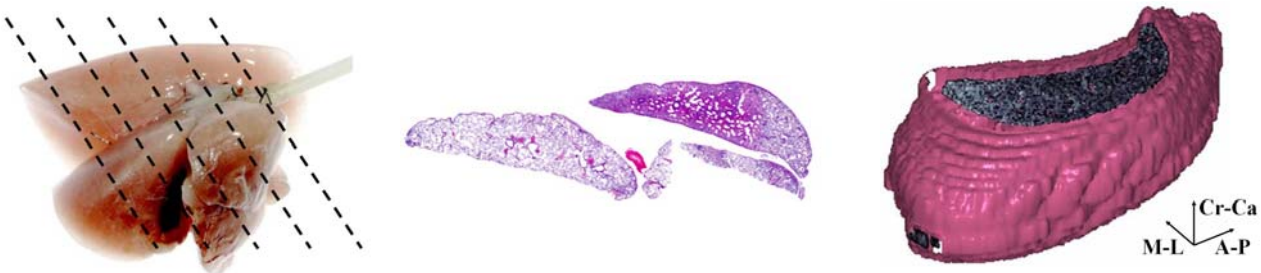


A. B. C.

Figure 1. Overview, study methodology. *A*. Dotted lines represent sample serial sections of excised lung tissue collected 48 hours post-insult. *B*. Exemplar image of histology section. *C*. Total lung reconstruction of centroid-aligned images. Triad shows Anterior-Posterior (A-P), Medial-Lateral (M-L) and Cranial-Caudal (Cr-Ca) directions.

Images were segmented to categorize the lung pixels into three masks: 1. healthy lung tissue, 2. pathologic lung tissue, and 3. blood. The parameters used in this algorithm are outlined in Table A1. The segmentation began by determining the quantity of blood in the image. Blood in a given image resulted from the presence of an arterial cross-section or bleeding following the insult. Since it was identifiable by a fairly homogenous RGB range, multi-channel thresholding was used to identify these pixels. Boolean operations were used to remove these pixels from the lung mask. A combination of morphological and filtering operations were then used to identify regions of pathology within the lung mask. The morphological operations used a combination of dilatation and erosion operations on the monochrome image to accentuate regions of pathology. A circular-average filtering operation was then applied to the image to smooth contrast within of the image. A gray-scale threshold was then applied to the processed, monochrome image. Pixels exceeding this

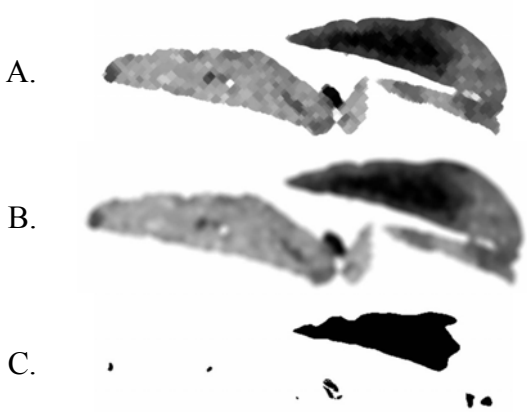


Figure 2. Segmentation process for pathologic tissue. *A*. Image after morphologic operation. *B*. Image after filtering operation. *C*. Image after thresholding operation. This binary image shows only pathology. The native is in Figure 1B.

threshold were considered areas of pathologic tissue. A Boolean operation was used to separate the pathologic lung tissue from the remaining lung mask, Figure 2.

## RESULTS

The results of the study are summarized in Table A2. The subjects experienced similar lung insults and were within a tight weight range (CoV, weight = 5.7%). While the distance between sections (Δ) were uniform for the right and the left sides, the number of sections per individual varied slightly. To aid in comparisons across modalities, pathology volumes identified by the algorithm were normalized to the total volume of the lung on a given side. The precisely quantified image resolution and slice interval enabled volumetric calculations of the segmented histology data. It was assumed that the composition of the section was uniform across Δ. The fraction of contusion determined by the algorithm varied across study subjects, but was always greatest on the struck side. The volume of pathology exceeded the volume of blood for all subjects. Normalized pathology from histology data were calculated taking the ratio of pathology *plus* blood pixel volumes to total lung pixel volumes.

CT data acquired just prior to sacrifice were segmented using a semi automated approach as part of a larger study. (Gayzik, 2007B) The fraction of pathology normalized to the right lung volume from CT are included in Table A2 and are shown with the histology data in Figure 3. The histology and CT segmentation approaches agree in that the volume of pathology from subjects 1 and 4 is greater than that in subjects 2 and 3. The total lung volume calculated from histology data was greater than that determined through CT segmentation for all subjects.

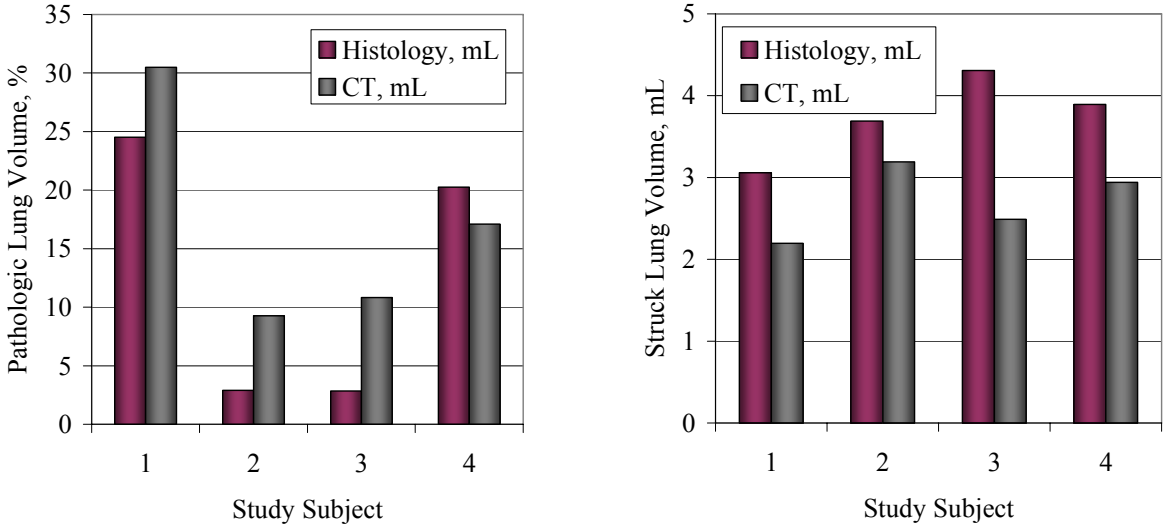


Figure 3. Comparison of results, histology vs. CT for struck lung. *A*. Volume of pathology normalized by total lung volume. *B*. Struck lung volume.

This study presented an automated algorithm for quantifying the volume of contusion in histological samples of H&E-stained rat lung. Digital histology analysis has become more common as increases in computational resources have allowed for fast and inexpensive

processing of high-resolution images. Applications of this approach are numerous. Corneal opacity, (Li, 2003) regional variation of patellar trabeculae, (Toumi, 2006) and tumor invasion and propagation (Ding, 2005; Akella, 2006) have all been quantified using a similar approach. The results of this study are encouraging. With respect to the model for PC itself, far more pathology was detected than blood in the tissue samples when comparing gross volumes. This indicates that the method used to elicit contusion is good for generating a blunt rather than penetrating injury mechanism. The data also suggest (Table A2, rows 1 and 13) that a relationship may exist between impact energy and pathology volume in the stuck lung. Further studies would be needed to establish significance between these values.

The primary motivation for this study was to compare normalized pathology data from the same subjects across two different modalities; Histology and CT. The results reflected similar trends in the data (Figure 3A). Mean pathology did not differ significantly between histology and CT ($p = 0.18$, paired t-test for sample means, $\alpha = 0.05$). For two of the study subjects ($N^{os.}$ 1 and 4) the Histology and CT segmentation found differences in the normalized contusion volume of 6% or less. But in the remaining subjects, the discrepancy between modalities was greater. This may be due to a number of factors. The total volume from the excised tissue (histology data) was greater than the total volume from CT segmentation (Figure 3B). This may be the result of quasi-static inflation of the excised tissue beyond its average *in-situ* volume. The implication of this over expansion is that it may have violated an implicit assumption of equal aeration between pathologic and healthy tissue. In addition, the CT pathology may reflect a variety of pathologic conditions beyond contusion, such as edema and atelectasis. These conditions work to increase the differences between the values determined by the two modalities.

Despite these discrepancies this study outlines a useful approach for improving histology and CT-based segmentation of PC and other pathologies since both the data sets were from the same individuals, collected at the same time, and experienced the same insult. In a previous study, the results of the histology analysis algorithm compared favorably to manual segmentation by a pathologist, exhibiting excellent specificity ($0.99 \pm 0.009$). (Gayzik, 2007A) The algorithm's sensitivity to contusion was less however, ($0.57 \pm 0.26$). This suggests that the algorithm could be improved through optimization of the parameters in Table A1. Future research will focus on optimizing these parameters to best match the pathologist and CT data, and to determine which parameters have the largest effect on the resulting estimates of pathology.

## CONCLUSIONS

An image analysis algorithm was developed to determine the normalized volume of pathology in histology from four contused lung specimens. Normalized pathology from CT of the same animals from a previous study, taken at the same time point, were used to compare results. The histology analysis algorithm and CT data found similar trends between individuals. The total lung volume estimated via histology was greater than that estimated using CT in all cases, and the fraction of pathologic lung calculated from CT was greater than that calculated from histology in 3 of 4 cases. Future efforts will focus on optimizing the parameters of the segmentation algorithm to improve this match. In conclusion, this approach represents a useful

method for improving the accuracy of both histology-based and CT-based segmentation processes.

## ACKNOWLEDGEMENTS

This publication was supported by Grant Number 1 R49 CE000664-01 from the Centers for Disease Control and Prevention (CDC). Its contents are solely the responsibility of the authors and do not necessarily represent the official views of the National Center for Injury Prevention and Control. Digital photography services provided by Creative Communications, Wake Forest University Baptist Medical Center, Winston-Salem, NC. Histology services provided by Harris Histology, Greenville, NC.

## REFERENCES

AKELLA, N. S., DING, Q. et al. (2006). A novel technique to quantify glioma tumor invasion using serial microscopy sections. J Neurosci Methods, 153(2): 183-9.

BLANSFIELD, J., DANIS, D. et al. (1999). Manual of Trauma Care: The First Hour. St. Louis, MO, Mosby.

COHN, S. M. (1997). Pulmonary contusion: review of the clinical entity. J Trauma 42(5): 973-9.

DING, Q., GRAMMER, J.R. et al. (2005). p27Kip1 and cyclin D1 are necessary for focal adhesion kinase regulation of cell cycle progression in glioblastoma cells propagated in vitro and in vivo in the mouse brain. J Biol Chem 280(8): 6802-15.

GAYZIK, F. S., BROWNLEE, N. A. et al. (2007A). An image analysis method for quantifying pulmonary contusion in histologic specimens. Southeast Bioengineering Conference, Duke University.

GAYZIK, F. S., HOTH, J. J. et al. (2007B). A finite element based injury metric for pulmonary contusion: Investigation of candidate injury metrics through correlation with computed tomography. Stapp Car Crash Journal 51: 189-209.

HOTH, J. J., STITZEL, J.D. et al. (2006). The pathogenesis of pulmonary contusion: an open chest model in the rat. J Trauma 61(1): 32-44; discussion 44-5.

LI, J. J., XU, L. et al. (2003). The application of digital photography with retroillumination for lens in cataract study. *Zhonghua Yan Ke Za Zhi* 39(5): 278-82. (English Abstract)

MILLER, P. R., CROCE, M. A., et al. (2001). ARDS after pulmonary contusion: accurate measurement of contusion volume identifies high-risk patients. J Trauma 51(2): 223-8; discussion 229-30.

STITZEL, J., GAYZIK, F. S., et al. (2005). Development of a finite element based injury metric for pulmonary contusion, Part I: model development and validation. Stapp Car Crash Journal 49: 271-289.

TOUMI, H., HIGASHIYAMA, I., et al. (2006). Regional variations in human patellar trabecular architecture and the structure of the proximal patellar tendon enthesis. J Anat 208(1): 47-57.

## APPENDIX

Table A1. Thresholding parameters used to segment blood, pathologic lung tissue and healthy lung tissue

| **Blood mask** | | **Pathology mask** | |
|---|---|---|---|
| **Channel** | **Range (inclusive)** | **Operation** | **Description** |
| Red | (197-240) | Morphologic | Diamond sampling element, 4 pixel axis |
| Green | (0-90) | Filter | Circular element, 5 pixel radius |
| Blue | (115-154) | Threshold (0-255) | 85 |

Table A2. Study results, all data collected 48 hours post-insult, the right lung was struck

| **Subject No.** | **1** | **2** | **3** | **4** | **Mean ± S.D.** |
|---|---|---|---|---|---|
| **Impact Experiment Data (Gayzik, 2007B)** | | | | | |
| Impact Energy, mJ | 9.91 | 5.23 | 8.95 | 13.1 | 9.29 ± 3.23 |
| Weight, gr | 364 | 389 | 339 | 373 | 366 ± 20.9 |
| **Histology Data** | | | | | |
| Distance Between Samples, Right, Δ, mm | 1.5 | 1.5 | 1.5 | 1.5 | |
| Number Sections, Right | 37 | 45 | 55 | 50 | |
| Distance Between Samples, Left, Δ, mm | 3.0 | 3.0 | 3.0 | 3.0 | |
| Number Sections, Left | 23 | 25 | 30 | 24 | |
| Image Resolution, mm/pixel | 0.021 | 0.021 | 0.021 | 0.021 | |
| Total Lung Volume, ml | 5.61 | 6.37 | 7.36 | 6.37 | 6.43 ± 0.72 |
| Right Lung Volume, ml | 3.06 | 3.69 | 4.31 | 3.89 | 3.74 ± 0.52 |
| Right Lung Pathology, ml | 0.745 | 0.103 | 0.106 | 0.759 | 0.428 ± 0.37 |
| Right Lung Blood, ml x $10^{-3}$ | 5.46 | 3.96 | 16.8 | 28.7 | 14.0 ± 12.0 |
| Pathology and Blood, Right, % | 24.5 | 2.90 | 2.85 | 20.3 | 12.63 ± 11.4 |
| Left Lung Volume, ml | 2.55 | 2.68 | 3.06 | 2.47 | 2.69 ± 0.26 |
| Left Lung Pathology, ml | 0.0669 | 0.0534 | 0.0270 | 0.0823 | 0.057 ± 0.02 |
| Left Lung Blood, ml x $10^{-3}$ | 1.64 | 6.83 | 16.3 | 8.70 | 8.36 ± 6.0 |
| Pathology and Blood, Left, % | 2.69 | 2.25 | 1.41 | 3.69 | 2.51 ± 0.95 |
| **CT Data (Gayzik, 2007B)** | | | | | |
| Slice Thickness, mm | 0.625 | 0.625 | 0.625 | 0.625 | |
| Image Resolution, mm/pixel | 0.190 | 0.190 | 0.190 | 0.190 | |
| Right Lung Volume, ml | 2.20 | 3.19 | 2.49 | 2.94 | 2.70 ± 0.45 |
| Total Lung Volume, ml | 4.05 | 5.57 | 5.25 | 4.99 | 4.97 ± 0.65 |
| Pathology, Right, % | 30.5 | 9.26 | 10.8 | 17.1 | 16.92 ± 9.66 |

## AUTHOR LIST

1. F. Scott Gayzik
   Medical Center Blvd., MRI 2, Winston-Salem, NC 27157
   336-716-6643
   sgayzik@wfubmc.edu

2. J. Jason Hoth
   Medical Center Blvd, Winston-Salem, NC 27157
   336-716-3813
   jhoth@wfubmc.edu

3. Noel A. Brownlee
   Medical Center Blvd., Winston-Salem, NC 27157
   336-716-3813
   nbrownle@wfubmc.edu

4. Joel D. Stitzel
   Medical Center Blvd., MRI 2, Winston-Salem, NC 27157
   336-716-5597
   jstitzel@wfubmc.edu